SCIENTIFIC REPORTS

OPEN

Masking of a circadian behavior in larval zebrafish involves the thalamo-habenula pathway

Received: 27 January 2017
Accepted: 10 May 2017
Published online: 22 June 2017

Qian Lin[1,6] & Suresh Jesuthasan[2,3,4,5]

Changes in illumination can rapidly influence behavior that is normally controlled by the circadian clock. This effect is termed masking. In mice, masking requires melanopsin-expressing retinal ganglion cells that detect blue light and project to the thalamus. It is not known whether masking is wavelength-dependent in other vertebrates, nor is it known whether the thalamus is also involved or how it influences masking. Here, we address these questions in zebrafish. We find that diel vertical migration, a circadian behavior in larval zebrafish, is effectively triggered by blue, but not by red light. Two-photon calcium imaging reveals that a thalamic nucleus and a downstream structure, the habenula, have a sustained response to blue but not to red light. Lesioning the habenula reduces light-evoked climbing. These data suggest that the thalamo-habenula pathway is involved in the ability of blue light to influence a circadian behavior.

Light has profound effects on animal behavior, independent of visual perception. One effect is to influence locomotor activity that is normally under the control of the circadian clock[1–4]. For example, in diurnal animals such as squirrels, birds and fish, short exposure to light during the night can stimulate movement (positive masking) while exposure to darkness during the day inhibits movement (negative masking). Direct photic control of movement, or masking, is thought to fine-tune behavior and physiology, such that the animal can respond quickly to changes in the environment. The neural mechanisms underlying masking are unclear[5]. In mammals, masking involves melanopsin-expressing retinal ganglion cells (mRGCs) that are directly sensitive to irradiance, especially of blue light[6,7]. Thus, one approach to identifying neural circuits mediating masking is to examine the projections of mRGCs. By expressing ß-galactosidase[8] or Cre-recombinase[9] in the melanopsin locus of mice, or by using viral-mediated tracing[10], it has been shown that mRGCs innervate multiple targets such as the suprachiasmatic nucleus (SCN), olivary pretectal nucleus as well as thalamic nuclei including the intergeniculate leaflet (IGL) and ventral lateral geniculate nucleus (vLGN). Lesions of the thalamus[11,12], but not of the SCN[13], have been reported to affect masking. This indicates an involvement of the thalamus in masking.

Brain regions downstream of the thalamus that contribute to masking are not defined. One approach to identifying these regions and the underlying mechanism of masking would be to carry out brain imaging using lighting conditions that elicit masking. Here, we do this using larval zebrafish, a system that allows imaging of neural activity across the entire brain at cellular resolution. We first ask whether masking in larval zebrafish[3] is dependent on wavelength. As a behavioral assay, we use diel vertical migration, which is the change in position within a water column that normally occurs over the course of a day; this movement may contribute to optimization of feeding and predator avoidance[14]. Like many other fish[14,15], larval zebrafish move to the top of a water column during the day, and to the bottom at night[16]. Diel vertical migration is absent in zebrafish larvae where melatonin production in the pineal has been disrupted, indicating that it is dependent on the circadian clock[16]. Vertical migration can also be affected by changes in light[17], suggesting that it can be masked. This would enable larvae to respond quickly to changes in light, for example climbing more rapidly to search for food when light is present. However, the wavelength dependency has not been reported. Here, we test this, and then image neural activity

[1]NUS Graduate School for Integrative Sciences and Engineering, 28 Medical Drive, National University of Singapore, Singapore, 117456, Singapore. [2]Lee Kong Chian School of Medicine, Nanyang Technological University, Singapore, 636921, Singapore. [3]Neural Circuitry and Behavior Laboratory, Institute of Molecular and Cell Biology, Singapore, 138673, Singapore. [4]Neuroscience and Behavioral Disorders Program, Duke-NUS Graduate Medical School, 8 College Road, Singapore, 169857, Singapore. [5]Department of Physiology, National University of Singapore, Singapore, 117597, Singapore. [6]Present address: The Rockefeller University, 1230 York Avenue, New York, NY 10065, USA. Correspondence and requests for materials should be addressed to S.J. (email: sureshj@ntu.edu.sg)

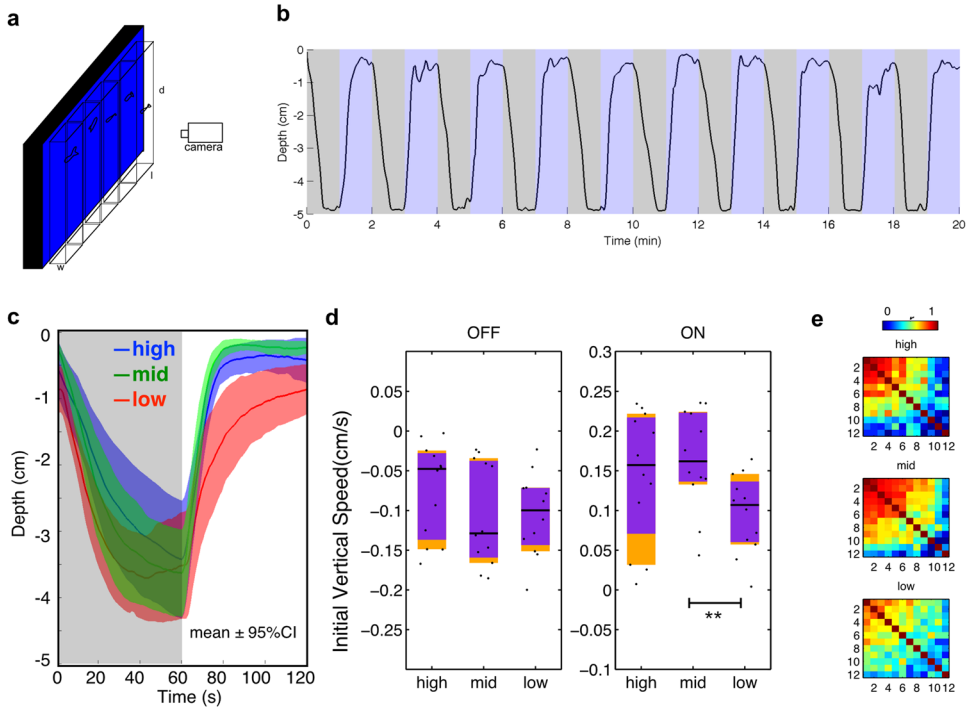

Figure 1. Blue light masks vertical migration. (**a**) Schematic of the assay. Larval zebrafish were placed individually in tanks in front of an LED backlight. (**b**) Response of 1 fish to ten cycles of blue (470 nm) light and darkness. (**c**) Depth of larvae across time under different intensities of blue light, averaged from 10 cycles. n = 12 for each group. Shadows indicate 95% confidence intervals (CIs). Mid-intensity 600 μW/cm^2, high-level 6000 μW/cm^2 and low-level is ~6 μW/cm^2. The photon intensity of mid-level is at the level of 10^{15} cm^{-2} s^{-1}. (**d**) Comparison of averaged initial 20 s vertical speed under different intensities of blue light. Horizontal black lines indicate median values, black dots show individual speeds, orange blocks show 95% CIs and purple blocks indicate the 25th and 75th percentiles. (**e**) Correlation coefficients of vertical position across time during 10 dark-light cycles under different intensities of light. Correlation matrices are different (mid vs high: $\chi^2 = 6519$, $df = 66$, $p < 0.0001$; mid vs low: $\chi^2 = 3963$, $df = 66$, $p < 0.0001$. Jennrich's χ^2 test[45]). For n = 3 groups, Bonferroni correction $\alpha = p/n = 0.05/3 = 0.0167$.

across the whole brain of larval zebrafish, to identify regions that may contribute to the control of movement by light.

Results

Vertical migration is effectively driven by blue light. To characterise vertical migration, larvae were placed independently in custom chambers (Fig. 1a) and exposed to 10 alternating periods of light and darkness, each lasting 1-minute. As previously reported[17], larval zebrafish moved upwards in the light and downwards in darkness (Fig. 1b). This behavior was induced by a range of intensities (Fig. 1c–e). Larvae showed different climbing speeds under different intensities (Kruskal-Wallis test $\chi^2 = 6.37$, $df = 2$, $p = 0.0414$ for climbing speed; $\chi^2 = 1.99$, $df = 2$, $p = 0.3693$ for diving speed). Larvae had a slower climbing speed under the low intensity compared to mid intensity (Mann-Whitney $U = 28$, $p = 0.006$, one tailed, rank-biserial correlation = 0.61). The vertical speeds under high and mid intensity were not different (light OFF: Mann-Whitney $U = 53$, $p = 0.28$, two tailed, rank-biserial correlation = 0.26; light ON: Mann-Whitney $U = 59$, $p = 0.52$, two tailed, rank-biserial correlation = 0.18). Low intensity of light caused a less robust climbing response, as indicated by the larger confidence interval (Fig. 1c), a lower occurrence rate (72 out of 120) and low correlation between the movements of individual fish (Fig. 1e). At the highest irradiance tested, slightly more fish responded in all trials (83 occurrences out of 120). The pair-wise correlation coefficients under mid-intensity light were higher than other light conditions ($\chi^2 = 9.81$, $df = 2$, $^{**}p = 0.0074$, Kruskal-Wallis test) and there were 88 occurrences. Mid vs high: $U = 2739$, $p = 0.0054$; Mid vs low: $U = 2803$, $^{**}p = 0.0022$, one tailed Mann-Whitney U test with Bonferroni correction. Thus, this condition was used subsequently.

Zebrafish have four cones[18], and are able to detect light across a broad region of the spectrum, from ultraviolet (UV)[19] to far red[20]. In rodents, UV-sensitive cones contribute to non-image forming response such as circadian photoentrainment and light-induced phase shift[21]. We thus tested whether UV light is able to mask vertical migration of larval zebrafish. Under UV light, at the same photon intensity as blue light, larvae frequently swam up and down, but these movements were not synchronized with periods of light and darkness (Fig. 2a,b). Most fish stayed at the lower portion of the water column during both light ON and OFF (Fig. 2b). UV light also led to lower mean vertical speeds (OFF & ON $^{***}p < 0.0001$, Mann-Whitney U test; Fig. 2c) and lower correlation coefficients ($^{***}p < 0.0001$; median $r = 0.11$ for UV light and 0.45 for blue light; Fig. 2d). This suggests that masking

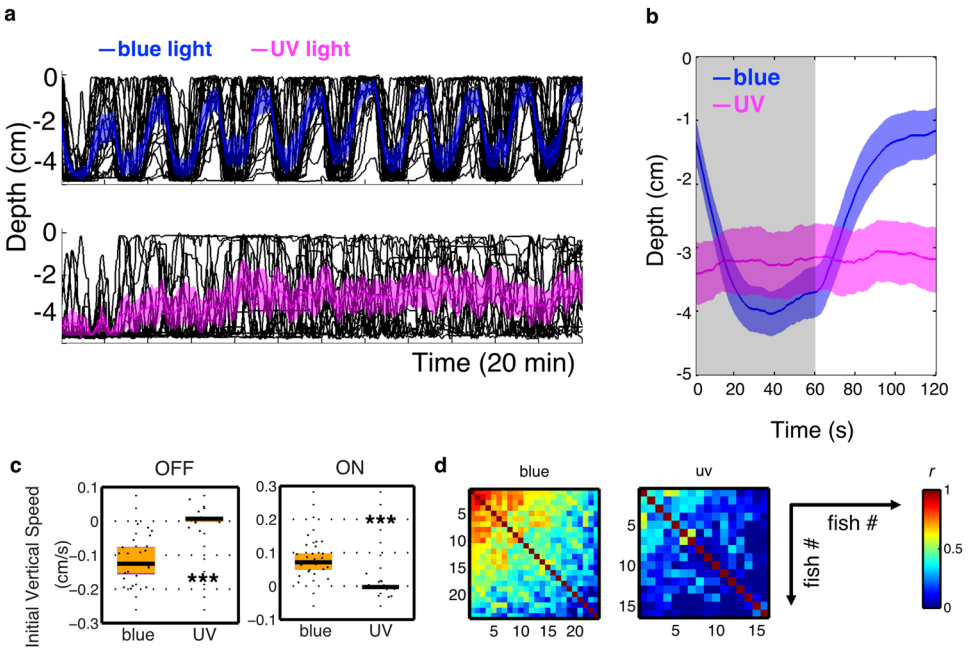

Figure 2. UV light fails to drive vertical migration. (**a**) Vertical migration of fish under blue (470 nm) and UV (375 nm) light at the same photon intensity, ~1.56×10^{15} cm^{-2} s^{-1}. Black lines represent individual trajectories, and colored traces represent the average of the group. Shadows indicate 95% confidence intervals. n = 24 for the blue group and n = 16 for the UV group. (**b**) Averaged vertical migration from 10 dark-light cycles. (**c**) Initial 20 s diving and climbing speed. Vertical speeds under UV are reduced relative to the speeds under blue light (light OFF: Mann-Whitney $U = 4$, $^{***}p < 0.0001$, two tailed, rank-biserial correlation = 0.98; light ON: Mann-Whitney $U = 6$, $^{***}p < 0.0001$, two tailed, rank-biserial correlation = 0.97). Horizontal black lines indicate median values, black dots show speed of individual fish, purple blocks show the 25th and 75th percentiles and orange blocks show 95% CIs. (**d**) Correlation coefficient of vertical position across time during 10 dark-light cycles. Correlation coefficient is lower under UV light than under blue light ($U = 3442$, $p < 0.0001$, one tailed Mann-Whitney U test; median $r = 0.11$ for UV and 0.45 for blue).

of vertical migration of larval zebrafish is not caused simply by a change in irradiance, but may be wavelength dependent.

To test this further, we examined the effects of red and green light, in comparison to blue. Under the same photon intensity, green light triggered a similar vertical migration as blue light, with similar depth over time (Fig. 3a,b), diving/climbing speeds (two-tailed $p > 0.7$; Fig. 3c), and high correlation coefficient across 10 cycles among individual fish (median $r = 0.67$ for blue, $r = 0.69$ for green; two-tailed $p = 0.53$; Fig. 3d). In contrast, red light failed to drive a full vertical migration (Fig. 3a,b), with a less synchronized up and down movement, causing a lower correlation coefficient among individuals (median $r = 0.40$, $^{**}p < 0.0001$; Fig. 3d). Fish also failed to remain at the top of the water column under red light (Fig. 3b), and there was decreased diving/climbing speeds (compared to blue light, diving: *one-tailed $p = 0.0097$; climbing: two-tailed $p = 0.040$; Fig. 3c). In addition, when the same photon intensity of red and blue light were given alternatively, larvae displayed a small but obvious vertical migration, diving upon red light onset and climbing upon blue light onset, leading to different vertical positions (**two-tailed $p = 0.008$; Fig. 3e). Thus, change in red light has distinct effects from change in green and blue light.

The deficits under red light could be because red light acts through a different light processing pathway that does not drive a full vertical migration response, or because the fish are less sensitive to red light. To investigate the latter possibility, red light of 10-fold higher in intensity was applied, to compensate for the reduced sensitivity. Under this higher intensity of red light, larvae still performed an incomplete vertical migration (Fig. 4a), with decreased depth during light onset (Fig. 4b), a decreased diving speed ($^{**}p = 0.004$; Fig. 4c), and lower synchronization among individuals (median Pearson's $r = 0.15$ in contrast to median $r = 0.45$ for blue; $p < 0.0001$; Fig. 4d). Although there was a similar climbing speed upon light onset (Fig. 4c), larval fish under bright red light did not maintain their vertical position during the light-on period (Fig. 4b). This different behavior implies that changes in blue and red illumination are not processed in the same way.

Calcium imaging identifies potential correlates of blue sensitivity. The difference between the effects of red and blue light provides a tool to probe the neural mechanism of masking. Specifically, neurons that are activated by changes in blue light, but not by changes in red light, are candidates for components of the circuits that mediate masking; cells that respond similarly could be those that detect visual stimuli in general. To identify these neurons, we performed calcium imaging of fish with broad expression of GCaMP6f[22], using resonant-scanning two-photon microscopy. Figure 5 shows the comparison of neural activity evoked by blue

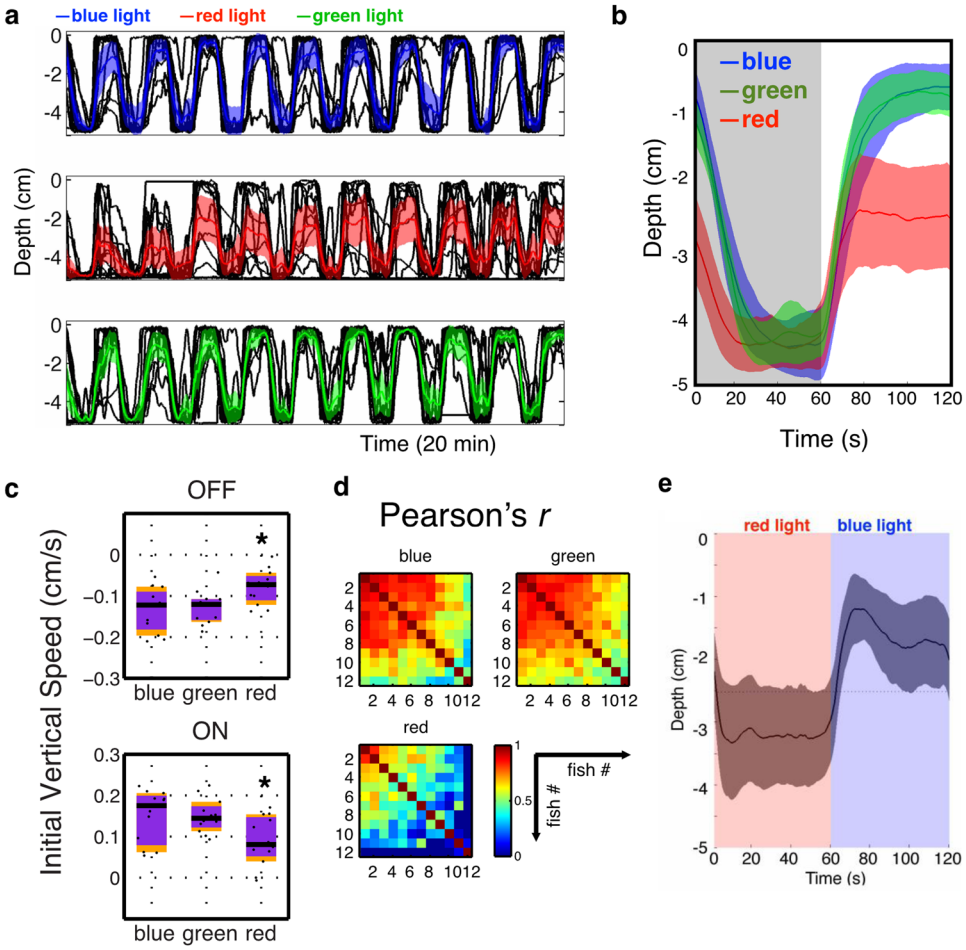

Figure 3. A comparison of vertical migration under blue, green and red light. (**a**) Vertical migration of larvae exposed to 10 cycles of blue (470 nm; 650 μW/cm^2), green (525 nm; 580 μW/cm^2) and red (660 nm; 465 μW/cm^2) light, which yield the same photon intensity, ~1.56×10^{15} cm^{-2} s^{-1}. Black lines represent individual fish, while colored traces represent the average. Shadows indicate 95% CIs. n = 12 for each group. (**b**) Mean vertical migration from 10 dark-light cycles, averaged from panel (a), represented as mean ± 95% CIs. (**c**) Comparisons of initial 20 s vertical swimming speeds. Vertical speeds under blue and green lights are similar (Diving: Mann-Whitney $U = 66$, $p = 0.76$, two tailed, rank-biserial correlation = 0.083; climbing: Mann-Whitney $U = 68$, $p = 0.84$, two tailed, rank-biserial correlation = 0.056). Vertical speeds under blue and red light are different (Diving: Mann-Whitney $U = 31$, $^*p = 0.0097$, one tailed, rank-biserial correlation = 0.60; Climbing: Mann-Whitney $U = 36$, $p = 0.040$, two tailed, rank-biserial correlation = 0.50). Vertical speeds under green and red light are different (Diving: Mann-Whitney $U = 30$, $p = 0.0083$, one tailed, rank-biserial correlation = 0.58 Climbing: Mann-Whitney $U = 34$, $p = 0.015$, one tailed, rank-biserial correlation = 0.53). (**d**) Correlation coefficient of vertical position across time during 10 dark-light cycles. Correlation matrices are different (blue vs green: $\chi^2 = 3288$, $df = 66$, $p < 0.0001$; blue vs red: $\chi^2 = 5534$, $df = 66$, $p < 0.0001$. Jennrich's χ^2 test). (**e**) Behavior under alternating red and blue light cycles with the same photon intensity ~1.56×10^{15} cm^{-2} s^{-1}, represented as mean ± 95% CIs. Larvae display vertical migration, with the vertical position under blue light being higher than the vertical position under red light (Mann-Whitney $U = 118$, $p = 0.008$, two tailed, rank-biserial correlation = 0.64, n = 12).

and red light. One-minute pulses of red or blue light, alternating with 1-minute darkness, were delivered in a random fashion. Images were processed by principal component analysis (PCA) to reduce dimensionality and then by independent component analysis (ICA) to obtain separate signals[23]. This analysis suggests that there are several responses to increase in irradiance. Blue-specific sustained excitation (Fig. 5c) was detected in the thalamus (Fig. 5a,b; blue pixels; arrowheads). A wavelength-independent transient excitation to onset and offset of light (Fig. 5d,e) was prominent in the tectal neuropil (pink and yellow pixels; Fig. 5a). Activity was also detected in the left habenula (Fig. 5a arrow), including sustained excitation to blue light and transient excitation to darkness.

Given that temporal signals derived from ICA were averaged by weights of each pixel, it is possible that real fluorescence signals might be different. To test this, ROIs were segmented from the ICA spatial maps by thresholding. The activities of individual ROIs were then averaged and presented as z-scores (Fig. 5g). Signals from segmented ROIs, such as the sustained excitation to blue light, were similar to their corresponding ICA temporal signals, indicating that ICA signals accurately reflect neural activity reported by the calcium indicator.

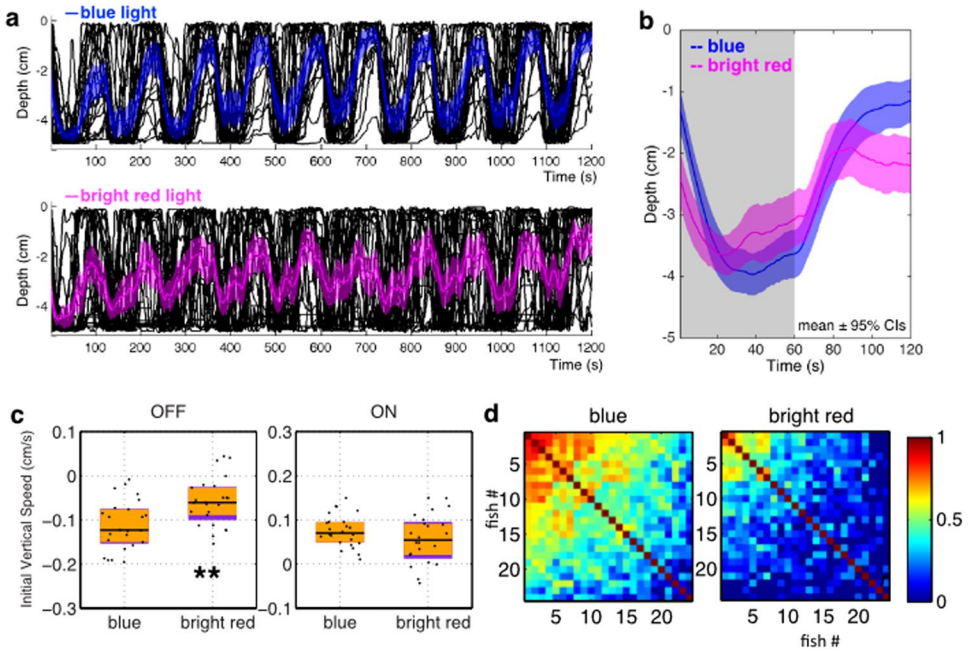

Figure 4. Blue and red light have different effects on vertical migration. (**a**) Vertical migration of fish under blue light and red light of ten-fold higher intensity: ~1.56×10^{15} cm^{-2} s^{-1} for blue light, and ~1.6×10^{16} cm^{-2} s^{-1} for red light. Black lines represent individual fish, and colored traces represent the average. Shadows indicate 95% CIs. Blue, 470 nm, 650 μW/cm^2; red, 660 nm, 4650 μW/cm^2. N = 24 for each group. (**b**) Averaged vertical migration from 10 dark-light cycles, averaged from panel. (**a**) Represented as mean ± 95% CIs. The curve under red light of high intensity is different from the one under blue towards the end of the light ON period. (**c**) Initial 20 s vertical swimming speed. Initial diving speeds upon light offset are different (Mann-Whitney $U = 145$, $^{**}p = 0.004$, two tailed, rank-biserial correlation = 0.50). Initial climbing speeds upon light onset are similar (Mann-Whitney $U = 231$, $p = 0.24$, two tailed, rank-biserial correlation = 0.20). Horizontal black lines indicate median values, black dots show speed of individual fish, purple blocks show the 25th and 75th percentiles and orange blocks show 95% CIs. (**d**) Correlation coefficient of vertical position across time during 10 dark-light cycles. Correlation matrices are significantly different ($\chi^2 = 12975$, $df = 276$, $p < 0.0001$. Jennrich's χ^2 test). Correlation coefficients are lower under red light of high intensity compared to blue light (median $r = 0.45$ for blue, 0.15 for red; $U = 2803$, $^{***}p < 0.0001$, one tailed Mann-Whitney U test).

To assess reproducibility, the neural responses of 7 fish were collected and integrated (Fig. 6; see Methods). Averaged ICA spatial maps show that the optic tectum has wavelength-independent phasic excitation in response to onset or offset of light (Fig. 6c,f). Darkness caused transient excitation in the optic tectum and the habenula (Fig. 6b,e). A sustained response to blue light was seen in the habenula and the thalamus (Fig. 6a,d).

Lesioning the habenula affects masking. The difference in habenula response to blue relative to red light suggests that the habenula may be involved in the effect of blue light on vertical migration. To test this, we recorded behaviour after lesioning the habenula. The zebrafish habenula has two major subdomains, dorsal and ventral, and dorsal subdomains are asymmetric. Imaging of the habenula with a galvano scanner, which provides a better signal-to-noise ratio, has shown that blue light evokes activity strongly in the dorsal left neuropil and also bilaterally in the ventral habenula[24]. We lesioned different regions of the habenula, using a femtosecond laser, to test their involvement in masking.

Fish with the dorsal left neuropil lesioned (Fig. 7a, Movie 1) displayed a decreased climbing speed in the presence of light ($U = 261$, one-tailed $p = 0.010$, rank-biserial correlation = 0.36), but diving speeds during darkness were not statistically different ($U = 329$, $p = 0.83$, rank-biserial correlation = 0.19) (Fig. 7b,c). Consistent with this, lesioned fish took a longer time to climb half of the water column during the light phase, while the time to dive half of the water column during the dark phase were not different (Fig. 7d). There was also a slight decrease in the correlation of movement (Fig. 7e; median $r = 0.45$ for the lesion group and 0.51 for the control group; $U = 63217$, $^{***}p < 0.0001$. N = 29 for control group, 28 for lesion group.). Lesioning the right dorsal neuropil (Fig. 7f) had no significant effects on the speed of diving during light OFF or climbing during light ON (Fig. 7g–I; light OFF: $U = 176$, $p = 0.268$, two tailed, rank-biserial correlation = 0.20; light ON: $U = 170$, $p = 0.208$, rank-biserial correlation = 0.23), but there was a difference in the correlation of movement (Fig. 7j; Median r = 0.41 for lesion group, 0.58 for control group. $U = 29200$, $^{***}p < 0.0001$. N = 21 for each group). When the ventral neuropils were lesioned (Fig. 7k; Movie 2), diving and climbing speeds differed significantly from control group (light OFF: $U = 219$, **one-tailed $p = 0.002$, rank-biserial correlation = 0.44; light ON: $U = 119$, $^{***}p < 0.0001$, rank-biserial correlation = 0.70). Swimming in the lesioned group was also less synchronized compared to the control group (Fig. 7o; median $r = 0.15$ for the lesion group and 0.51 for the control group; $U = 23885$, $^{***}p < 0.0001$; N = 29 for

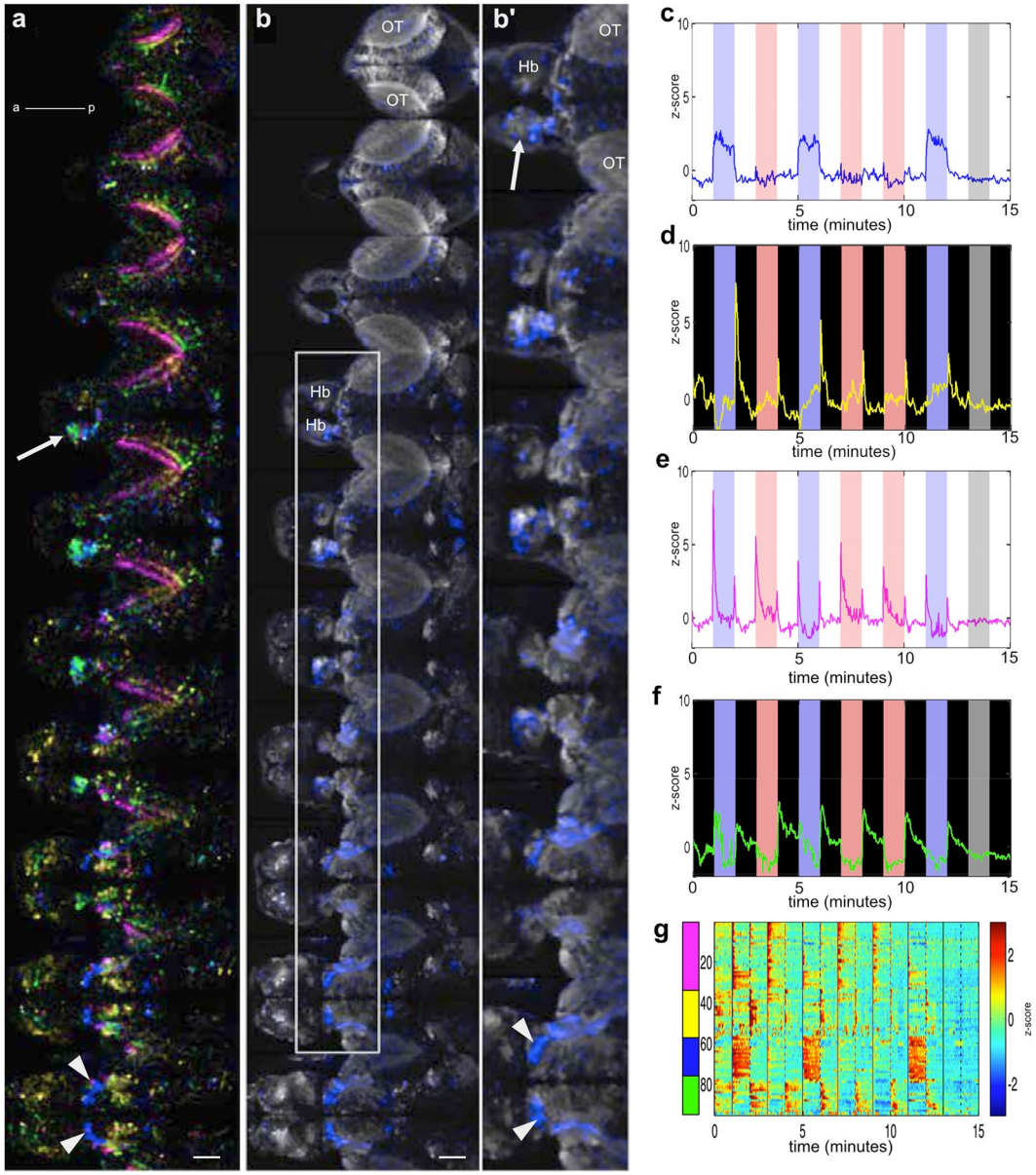

Figure 5. Overview of blue versus red light evoked activity in the brain. (**a**) Optical sections in a 6 dpf *elavl3:GCaMP6f* fish, going from dorsal to ventral. Each plane is separated by 10 µm. The area imaged at each plane is 443.47 µm x 222.73 µm. (**b**) Distribution of light-evoked activity in one fish, generated from ICA spatial maps. The white arrowheads indicate the thalamus, while the arrow indicates the habenula. (**b**) A magnified view of the area boxed in panel (b). **(c–f)** Different classes of responses, obtained by PCA followed by ICA. The same colours are used in panel (b). The blue and red bars indicate the periods that blue or red light was delivered. (**g**) Light-evoked activity in segmented ROIs, which were derived from ICA spatial maps. OT: optic tectum; Hb: habenula; a: anterior; p: posterior. Gamma of 0.65 was applied to panels (a and b). Scale bar = 50 µm.

control group, 27 for lesion group). These results are consistent with the hypothesis that the habenula is involved in the ability of blue light to mask diel vertical migration.

Discussion

In this manuscript, we provide evidence that blue light can drive vertical migration in larval zebrafish. This sensitivity to blue light may reflect the fact that shorter wavelengths of light penetrate water most readily, making sensitivity to blue light beneficial for innate responses. We also show that blue light stimulates a thalamic nucleus and the habenula. Dreosti *et al.*[25] have previously shown that a flash of light stimulates the zebrafish left habenula. We extend these results by showing that there is a wavelength-dependency in the habenula response. By lesioning, we show that the habenula influences the effect of blue light on vertical migration. As the thalamus directly innervates the habenula and appears to be the only pathway mediating the response of the habenula to light[24],

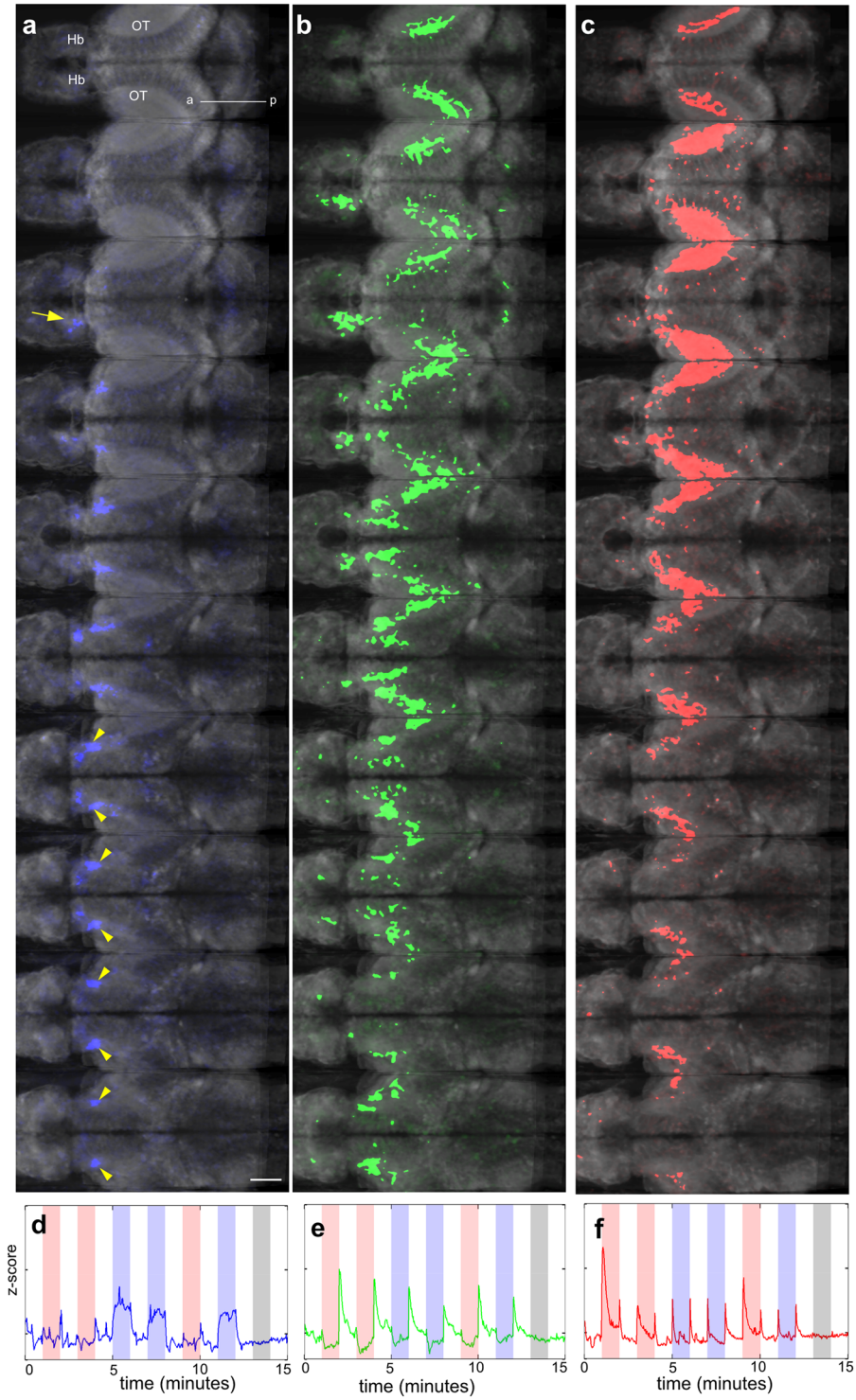

Figure 6. Averaged response of the brain to irradiance change. (**a–c**) Regions with sustained response to blue light (**a**), to offset of light (**b**) and to onset and offset of both blue and red light (**c**). The corresponding activity traces are shown in panels (d,e and f). These data are compiled from 7 fish.

these results indicate that a thalamo-habenula projection is involved in the ability of blue light to mask a circadian behavior. The lesioning did not fully abolish vertical migration, however. This may be due to limitations of lesioning – e.g. there was only partial loss of function – and the involvement of additional pathways. In particular, deep brain photoreceptors that contribute to the vertical migration[17,26] may operate independently of the thalamus.

The thalamic nucleus involved here may be the nucleus rostrolateralis[27,28], a retino-recipient structure that has been defined in fish, but whose homology to nuclei in the mammalian thalamus is undefined. Connectivity from this nucleus to the habenula has been shown by several groups[24,28,29]. The neuropil of the nucleus rostrolateralis

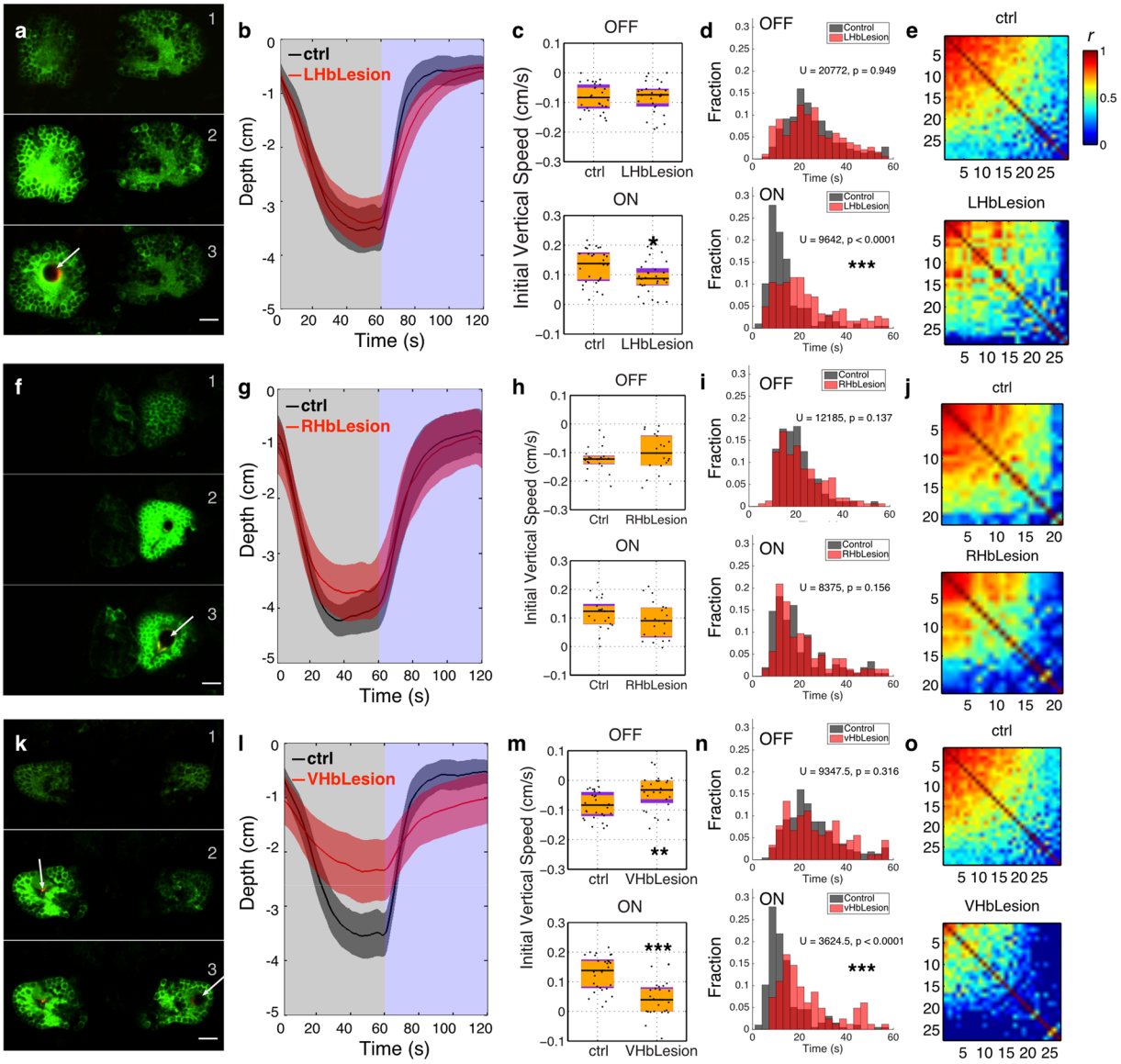

Figure 7. Lesion of the habenula inhibits masking of vertical migration. Effects of lesioning the left dorsal (**a**–**e**). N = 29 for control group, 28 for lesion group), right dorsal (**f**,**j**). N = 21 for each group) and ventral (**k**–**o**). N = 29 for control group, 27 for lesion group) habenula. (**a**,**f**,**k**) Stills from a time-lapse recording taken during the lesioning process, showing the habenula before (top), during (middle) and immediately after (bottom) lesioning. Lesioning leads to the formation of a bubble (arrow) and an extended rise in GCaMP3 fluorescence in surrounding cells. (**b**,**g**,**l**) Average position of fish during light ON and OFF. Shadows represent 95% CIs. (**c**,**h**,**m**) Initial vertical speed during light ON and OFF. Horizontal black lines indicate median values, black dots show individual fish, purple blocks show the 25th and 75th percentiles and orange blocks show 95% CIs. (**d**,**i**,**n**) Time taken to migrate half-way up or down the water column. The bars show the percentage of fish that reach this mark within the indicated time. (**e**,**j**,**o**) Correlation between the movement of individual fish.

may include the arborization field AF4[24,30]. AF4 is innervated by M3 and M4 retinal ganglion cells[31], which are both "ON" neurons. Based on the sustained, eye-dependent excitation in the thalamic neuropil in the presence of blue light[24], it is likely that some M3 or M4 neurons are either intrinsically sensitive to blue light[32]. This was confirmed recently by Zhang *et al.*[29], who showed that retinal ganglion cells innervating AF4 expressing *opn4xa*.

There are several lines of evidence to suggest that a thalamic nucleus with blue sensitivity and connectivity to the habenula is not a feature that is specific to larval fish. In the frog, electrical recordings have demonstrated a preferential response to blue light in the dorsal thalamus[33] and retrograde tracing shows that the frog habenula is innervated by the dorsal thalamus[34]. In the rat, anterograde tracing suggests that neurons from the thalamus innervate the habenula[35]. In humans, blue light activates the thalamus[36], which has functional connectivity with the habenula[37]. It is thus possible that a thalamo-habenula projection plays a role in the ability of blue light to mask behavior in many different vertebrates.

Methods

Zebrafish lines. Experiments were carried out in accordance with protocols approved by the Institutional Animal Care and Use Committee of the Biological Resource Centre at Biopolis, Singapore. Zebrafish (*Danio rerio*) lines used in this study were: *elavl3:GCaMP6f*[24], *s1011tGAL4*[38], *and UAS:GCaMP3*[39]. Experiments were carried on *nacre*$^{-/-}$ mutant fish, which are derived from an AB background[40]. Animals were housed in a facility with lights on between 8 am and 10 pm, and were chosen randomly for experiments.

Climbing assay. Naive larvae were placed individually in a chamber (3.0 cm length × 1.0 cm width X 5.0 cm height), and housed inside an incubator to exclude light. After 3–8 min adaptation to light, larvae were exposed to 10 cycles of alternating light/dark, each consisting of 60 seconds light ON and 60 seconds light OFF. Blue (470 nm peak), green (525 nm peak) or red light (660 nm peak) was provided by a LED backlight (TMS; see http://tms-lite.com/wavelength/ for spectra). Photon intensity, which is the relevant measure for the non-visual system[41], was calculated using the equation $I = P/(A*E)$. Power, P, was measured using a meter (ThorLabs PM100A) and A is the receptive area of the photodiode power sensor (Thorlabs S120VC). E, the energy of a single photon, was calculated with the equation $E = hc/\lambda$, where c is light velocity and h is Planck's constant.

6 fish were tested simultaneously. Videos were recorded at 5 fps, 640 × 480 pixel resolution, using MicroManager[42] to control a Grasshopper camera (Point Grey Research) equipped with a 12 mm lens and 830 nm longpass filter. Four infrared LED bars (TMS-lite, Model: LBS2-00-080-3-IR850-24V, 850 nm) were used for illumination. The light box was controlled by a power supply analogue (TMS-lite), which was triggered by a microcontroller board (Arduino UNO SMD) and Arduino software. All animals for a given experiment were from the same batch and from the same parents. Behavior experiments were carried out from 11 am-6 pm. Preliminary experiments indicate that animals respond similarly throughout this period (Supplementary Figure S1). Experiments reported here were performed on larvae aged 14–15 days post fertilization, as nacre larvae could be automatically tracked at this time. Preliminary experiments indicate that animals at a younger age respond similarly (Supplementary Figure S2).

No animals were excluded from analysis, which was performed using custom-written ImageJ[43] macros and Matlab codes that allowed automatic tracking following thresholding. Correlation coefficients (Pearson's r) were calculated using the *corrcoef* function in MATLAB (MathWorks). Sample size was chosen based on preliminary experiments, and on previous work with a similar assay[17]. No blinding was done, as a computer performed analysis automatically.

The first 20 seconds of each light/dark cycle was used to calculate initial swimming speed. The last 20-second window was used to compare vertical position. Results of vertical position during migration were presented as $(x \pm y)$ representing (mean ± 95% confidence interval (CIs)) to estimate the means of vertical positions of the population. Some data sets rejected the normality hypothesis as determined by the Shapiro-Wilk test. Therefore, all the pairwise comparisons were performed with the Mann-Whitney-U test, a non-parametric test, at a significance level of 0.05. $*p < 0.05$, $**p < 0.01$, $***p < 0.001$. The use of the one- or two-tail test is stated in the legend. For multiple comparisons, Kruskal-Wallis tests were performed first, followed by pairwise Mann-Whitney-U tests with the Bonferroni correction. For an experiment with N hypotheses with a desired $\alpha = 0.05$, the Bonferroni correction were performed on each individual hypothesis at $\alpha = 0.05/N$. $*p < 0.05/N$, $**p < 0.01/N$, $***p < 0.001/N$. Statistical test and data analysis were performed in MATLAB.

The use of multiple light-dark cycles represents technical replicates; the use of multiple animals represents biological replicates. The occurrence rate is defined as the number of cases where the fish reached the halfway point during a climb or dive.

To establish the appropriate intensity of blue light, three different light intensities were tested: 6 μW/cm^2, 600 μW/cm^2 and 6000 μW/cm^2. 600 μW/cm^2 was used in all subsequent experiments.

Two-photon calcium imaging. 5–6 dpf zebrafish larvae were first anaesthetized in mivacurium and then mounted in 1.5% low-melting-temperature agarose in a glass- bottom dish (Mat Tek) and immersed in E3 water. Fish were imaged on an upright Nikon resonant-scanning two-photon microscope (A1RMP), with a 25x water immersion objective (NA = 1.1) and the laser (Coherent Vision II) tuned to 960 nm. To image different z planes, a piezo drive (Mad City Labs) was used at a step size of 10 μm for light-evoked activity recording. The frame rate for whole brain imaging was 7.1 Hz (Fig. 2); each stack consisted of 10 frames. For light stimulus, the blue and red light boxes were controlled by a power supply unit (TMS-lite), triggered by a 5 V TTL signal from a National Instruments DAQ board that was controlled by the Nikon Elements software.

Green light could not be used as a stimulus in the imaging experiment, due to overlap with the emission spectrum of GCaMP6f.

Image analysis. For whole brain imaging data, principal component analysis (PCA) was used to reduce dimensions and independent component analysis (ICA) was used to separate independent signals. Matlab codes for these were adapted from a toolbox provided by Mukamel *et al.*[23]. Spatial maps from ICA were used to generate segmented regions of interest (ROIs), and temporal signals from ICA were used to calculate correlation (corr function in Matlab) to the stimuli and between different animals (correlation > 0.5 and p-value < 0.05 were used as threshold values).

Integration of calcium imaging data from multiple animals. 5 template signals were generated using square and sawtooth waves: square waves for blue onset and red onset; sawtooth waves for mixed onset, mixed offset and blue offset. The categories and shapes of the template signal were chosen based on observation from all fish data. Blue and red light pulses were delivered randomly. The timing of the templates was determined by the stimulus, and are different for different fishes. For an ICA temporal signal, the correlation coefficients against all

the 5 templates were computed and then the maximum was chosen. If the maximal correlation coefficient was larger than 0.5 (threshold chosen empirically), then this ICA signal, as well as its corresponding spatial map, was categorized. Finally, the ICA spatial maps, from different fish but belonging to the same categories, were registered by translation and then averaged in imageJ.

To verify that signals from a single fish did not disproportionately drive the averaged map, we plotted the responses in all fish individually (Supplementary Figures S3 and S4).

Code availability. Macros used in this study are available at https://github.com/LIN-Qian/Analysis_LightEvokedActivity.

Laser ablation. *s1011tGAL4, UAS:GCaMP3* larvae were anaesthetized and then mounted in 2% low-melting temperature agarose. Lesions were created with the IR laser tuned to 960 nm and fixed on a single point. Several pulses, each lasting 100–500 msec, were used. Lesioning was monitored by time-lapse imaging before and after each pulse, and was judged successful when there was a localized increase in GCaMP6f fluorescence and formation of a bubble[44]. To further characterize the lesion, a z-stack was collected.

References

1. Gander, P. H. & Moore-Ede, M. C. Light-dark masking of circadian temperature and activity rhythms in squirrel monkeys. *Am J Physiol* **245**, R927–34 (1983).
2. Aschoff, J. & Goetz, von, C. Masking of circadian activity rhythms in canaries by light and dark. *J. Biol. Rhythms.* **4**, 29–38 (1989).
3. Burgess, H. A. & Granato, M. Modulation of locomotor activity in larval zebrafish during light adaptation. *J Exp Biol* **210**, 2526–2539 (2007).
4. Redlin, U. & Mrosovsky, N. Masking of locomotor activity in hamsters. *J. Comp. Physiol. A* **184**, 429–437 (1999).
5. Redlin, U. Neural basis and biological function of masking by light in mammals: suppression of melatonin and locomotor activity. *Chronobiol. Int.* **18**, 737–758 (2001).
6. Mrosovsky, N. & Hattar, S. Impaired masking responses to light in melanopsin-knockout mice. *Chronobiol. Int.* **20**, 989–999 (2003).
7. Panda, S. *et al*. Melanopsin is required for non-image-forming photic responses in blind mice. *Science* **301**, 525–527 (2003).
8. Hattar, S. *et al*. Central projections of melanopsin-expressing retinal ganglion cells in the mouse. *J Comp Neurol* **497**, 326–349 (2006).
9. Ecker, J. L. *et al*. Melanopsin-expressing retinal ganglion-cell photoreceptors: cellular diversity and role in pattern vision. *Neuron.* **67**, 49–60 (2010).
10. Gooley, J. J., Lu, J., Fischer, D. & Saper, C. B. A broad role for melanopsin in nonvisual photoreception. *J Neurosci* **23**, 7093–7106 (2003).
11. Redlin, U., Vrang, N. & Mrosovsky, N. Enhanced masking response to light in hamsters with IGL lesions. *J. Comp. Physiol. A.* **184**, 449–456 (1999).
12. Gall, A. J., Smale, L., Yan, L. & Nunez, A. A. Lesions of the Intergeniculate Leaflet Lead to a Reorganization in Circadian Regulation and a Reversal in Masking Responses to Photic Stimuli in the Nile Grass Rat. *PLoS ONE* **8**, e67387 (2013).
13. Redlin, U. & Mrosovsky, N. Masking by light in hamsters with SCN lesions. *J. Comp. Physiol. A* **184**, 439–448 (1999).
14. Brodeur, R. D. & Rugen, W. C. Diel vertical distribution of ichthyoplankton in the northern Gulf of Alaska. *Fishery Bulletin* (1994).
15. Neilson, J. D. & Perry, R. I. Diel vertical migrations of marine fishes: an obligate or facultative process? *Advances in marine biology.* **26**, 115–168 (1990).
16. Ben-Moshe Livne, Z. *et al*. Genetically Blocking the Zebrafish Pineal Clock Affects Circadian Behavior. *PLoS Genet.* **12**, e1006445–26 (2016).
17. Fernandes, A. M. *et al*. Deep brain photoreceptors control light-seeking behavior in zebrafish larvae. *Curr Biol.* **22**, 2042–2047 (2012).
18. Hughes, A., Saszik, S., Bilotta, J., Demarco, P. J. & Patterson, W. F. Cone contributions to the photopic spectral sensitivity of the zebrafish ERG. *Visual Neuroscience.* **15**, 1029–1037 (1998).
19. Endeman, D., Klaassen, L. J. & Kamermans, M. Action spectra of zebrafish cone photoreceptors. *PLoS ONE* **8**, e68540 (2013).
20. Shcherbakov, D. *et al*. Sensitivity differences in fish offer near-infrared vision as an adaptable evolutionary trait. *PLoS ONE* **8**, e64429 (2013).
21. van Oosterhout, F. *et al*. Ultraviolet light provides a major input to non-image-forming light detection in mice. *Curr Biol.* **22**, 1397–1402 (2012).
22. Chen, T.-W. *et al*. Ultrasensitive fluorescent proteins for imaging neuronal activity. *Nature.* **499**, 295–300 (2013).
23. Mukamel, E. A., Nimmerjahn, A. & Schnitzer, M. J. Automated analysis of cellular signals from large-scale calcium imaging data. *Neuron.* **63**, 747–760 (2009).
24. Cheng, R.-K. *et al*. The thalamus drives light-evoked activity in the habenula of larval zebrafish. *bio Rxiv*. doi:10.1101/047936 (2016).
25. Dreosti, E., Vendrell-Llopis, N., Carl, M., Yaksi, E. & Wilson, S. W. Left-right asymmetry is required for the habenulae to respond to both visual and olfactory stimuli. *Curr Biol* **24**, 440–445 (2014).
26. Horstick, E. J., Bayleyen, Y., Sinclair, J. L. & Burgess, H. A. Search strategy is regulated by somatostatin signaling and deep brain photoreceptors in zebrafish. *BMC Biology. 2015 13:1* **15**, 4 (2017).
27. Saidel, W. M. Nucleus Rostrolateralis: An Expansion of the Epithalamus in Some Actinopterygii. *The Anatomical Record* **296**, 1594–1602 (2013).
28. Turner, K. J. *et al*. Afferent Connectivity of the Zebrafish Habenulae. *Front Neural Circuits* **10**, 3512 (2016).
29. Zhang, B.-B., Yao, Y.-Y., Zhang, H.-F., Kawakami, K. & Du, J.-L. Left Habenula Mediates Light-Preference Behavior in Zebrafish via an Asymmetrical Visual Pathway. *Neuron.* **93**, 914–928.e4 (2017).
30. Burrill, J. D. & Easter, S. S. Development of the retinofugal projections in the embryonic and larval zebrafish (Brachydanio rerio). *J Comp Neurol.* **346**, 583–600 (1994).
31. Robles, E., Laurell, E. & Baier, H. The retinal projectome reveals brain-area-specific visual representations generated by ganglion cell diversity. *Curr Biol.* **24**, 2085–2096 (2014).
32. Matos-Cruz, V. *et al*. Unexpected diversity and photoperiod dependence of the zebrafish melanopsin system. *PLoS ONE* **6**, e25111 (2011).
33. Muntz, W. R. Microelectrode recordings from the diencephalon of the frog (Rana pipiens) and a blue-sensitive system. *J Neurophysiol.* **25**, 699–711 (1962).
34. Kemali, M., Guglielmotti, V. & Gioffré, D. Neuroanatomical identification of the frog habenular connections using peroxidase (HRP). *Exp Brain Res.* **38**, 341–347 (1980).
35. Moore, R. Y., Weis, R. & Moga, M. M. Efferent projections of the intergeniculate leaflet and the ventral lateral geniculate nucleus in the rat. *J Comp Neurol.* **420**, 398–418 (2000).

36. Vandewalle, G. *et al*. Wavelength-Dependent Modulation of Brain Responses to a Working Memory Task by Daytime Light Exposure. *Cereb. Cortex.* **17**, 2788–2795 (2007).
37. Torrisi, S. *et al*. Resting State Connectivity of the Human Habenula at Ultra-High Field. *Neuroimage* 1–21, doi:10.1016/j.neuroimage.2016.10.034 (2016).
38. Scott, E. K. & Baier, H. The cellular architecture of the larval zebrafish tectum, as revealed by gal4 enhancer trap lines. *Front Neural Circuits.* **3**, 13 (2009).
39. Scott, E. K. *et al*. Targeting neural circuitry in zebrafish using GAL4 enhancer trapping. *Nat Methods.* **4**, 323–326 (2007).
40. Lister, J. A., Robertson, C. P., Lepage, T., Johnson, S. L. & Raible, D. W. nacre encodes a zebrafish microphthalmia-related protein that regulates neural-crest-derived pigment cell fate. *Development.* **126**, 3757–3767 (1999).
41. Vandewalle, G., Maquet, P. & Dijk, D.-J. Light as a modulator of cognitive brain function. *Trends Cogn Sci (Regul Ed)* **13**, 429–438 (2009).
42. Edelstein, A., Amodaj, N., Hoover, K., Vale, R. & Stuurman, N. *Computer Control of Microscopes Using μManager*. 14.20.1–14.20.17, doi:10.1002/0471142727.mb1420s92(John Wiley & Sons, Inc., 2001).
43. Schneider, C. A., Rasband, W. S. & Eliceiri, K. W. NIH Image to ImageJ: 25 years of image analysis. *Nat Methods.* **9**, 671–675 (2012).
44. Venugopalan, V., Guerra, A., Nahen, K. & Vogel, A. Role of Laser-Induced Plasma Formation in Pulsed Cellular Microsurgery and Micromanipulation. *Phys. Rev. Lett.* **88**, 078103 (2002).
45. Jennrich, R. I. An Asymptotic $\chi 2$ Test for the Equality of Two Correlation Matrices. *Journal of the American Statistical Association* **65**, 904 (1970).

Acknowledgements

This work was supported by core funding from the Institute of Molecular and Cell Biologyand a Lee Kong Chian School of Medicine, Nanyang Technological University MOE Start-Up Grant to SJ. QL was supported by a NGS fellowship from the National University of Singapore.

Author Contributions

Q.L. designed and performed experiments, analysed data and prepared all Figures. S.J. designed experiments and wrote the manuscript. Both authors reviewed the manuscript.

Additional Information

Supplementary information accompanies this paper at doi:10.1038/s41598-017-04205-7

Competing Interests: The authors declare that they have no competing interests.

Publisher's note: Springer Nature remains neutral with regard to jurisdictional claims in published maps and institutional affiliations.